Potential dependent selective dissolution of Ti–6Al–4V and laser treated Ti–6Al–4V in acid/chloride media

M.M. KHALED

King Fahd University of Petroleum and Minerals, Department of Chemistry, Dhahran 31261, Saudi Arabia
(e-mail: mkhaled@kfupm.edu.sa or mazenkhaled@hotmail.com)

Abstract

The corrosion properties of Ti–6Al–4V and laser surface melted (LSM) Ti–6Al–4V samples were investigated in 0.05 M H_2SO_4/0.05 M NaCl solution. Laser surface treatment was found to increase the corrosion potential and decrease the corrosion rates of the alloy. The current–potential profile of the LSM was found to be generally noisy below 0.5 V, indicating an unstable surface, which undergoes continuous dissolution and repassivation. However, above 0.5 V the LSM specimen exhibited higher corrosion current compared to the untreated alloy. Inductively coupled plasma (ICP) analysis of metals in solution was carried out after controlled potential electrolysis. Generally, the aluminium percentage was found to be the highest in solution compared to titanium and vanadium. The aluminium percentage in solution reached 94% compared to titanium and vanadium upon polarization in the passive region at 1.01 V. SEM showed that some local and shallow pitting to occur in both the untreated and LSM alloy. EDS results showed that aluminium composition of the electrolysed alloy surface is lower than the original material composition, and decreased from 6% in the original alloy to 0.18% after two hours of electrolysis of the LSM specimen.

1. Introduction

Ti–6A1–4V is an important alloy in engineering. It was developed in the early 1950s for aerospace applications due to its high strength-to-density ratios [1, 2]. Its excellent resistance to corrosion, particularly in oxidizing and chloride-containing process streams, extended its usage to a variety of industrial processes. The corrosion resistance is mainly due to the formation of very stable, continuous, highly adherent, and protective oxide films. The oxide film has been shown to consist mainly of TiO_2, in addition to a mixture of other oxides such as Ti_2O_3 and TiO [3, 4].

Despite the fact that the oxide film is typically less than 10 nm thick, it is highly chemically resistant. For instance, the alloy is used for handling nitric acid in industrial applications and corrosive environments. The alloy is attacked by very few substances including hot hydrochloric acid, sulfuric acid, sodium hydroxide and hydrogen fluoride. Despite the excellent corrosion properties of the alloy, it suffers from poor wear resistance which is needed, for instance, in turbines and implants. Surface modification is needed to improve the tribological, wear and corrosion properties of the alloy [5, 6]. Many techniques are available to improve the tribological properties of the alloy surface to make it more resistive to wear and corrosion. One of the promising

techniques relies on the use of lasers to modify the surface structures and composition [7]. Recently studies have shown laser surface melting improve the surface properties and corrosion resistance of metallic surfaces for different engineering and biomedical applications [8–12].

Byproducts of wear are a serious problem in the implants industry. It was found, for instance, that metallic ions released *in vitro* are cytotoxic, in titanium-base [13] and cobalt–chromium alloys [14]. Another study found that patients on chronic renal hemodialysis may develop systematic aluminium toxicity manifested as aluminium-associated osteomalacia [15]. The aluminium ion is similar in size to the ferric ion and smaller than magnesium and calcium ions and hence aluminium can replace magnesium in many biological systems and it competes with calcium for phosphate and small ligands [16]. In addition, the aluminium ion binds with anions much more strongly than the biological metals. Aluminium binds ATP 10^7 times more strongly than magnesium, thus interfering with reactions that require readily reversible dissociation [17].

Aluminium produces toxic effects at the cell membrane by altering the physical properties of the membrane, by interfering with the function of voltage-activated ionic channels, and by altering the secretion of transmitters. Ti–6Al–4V alloy contains 6% aluminium

and is used in hip replacement, facial implants and dentistry.

Recently it has been shown that laser treated and coated Ti–6Al–4V improved the corrosion resistance of the alloy as deduced from electrochemical measurements [18]. The study showed that upon electrolysis in acid/chloride solution the aluminium metal leaches selectively at approximately 90% ion concentration in the electrolysed solution compared to titanium and vanadium. The goal of this paper is to investigate the potential dependent leaching of the alloy constituents as a function of applied potential and duration prior and after laser treatment. Potential step electrolysis was carried out on the laser surface treated and untreated specimen. The potentials were selected to reflect the different electrochemical regions of the potentiodynamic curve. The three ions Ti, Al and V were measured after 30 min and 2 h of electrolysis.

2. Experimental details

A commercial Ti–6Al–4V alloy consisting of α and β phases, was used as the workpiece material. The alloy composition is given in Table 1. The workpieces were prepared from rectangular dimensions of 40 mm $\times$ 12 mm $\times$ 2 mm.

A CO_2 laser with nominal output power of 1.6 kW was used to irradiate the workpiece. A 100 mm focal length lens was used to focus the laser beam. Nitrogen at very low pressure was introduced coaxially with the laser beam to minimize high temperature oxidation reactions during the laser processing. The workpiece speed was kept constant at 0.3 m s^{-1}. The laser beam was defocused by changing the focus setting of the focusing lens to obtain a power intensity of the order of 10^5 W cm^{-2} at the workpiece surface. The laser treated workpiece had a rippled surface appearance. Consequently the laser treated surfaces were polished lightly with a diamond paste of grade 0.1 μm to obtain the maximum surface roughness of the order of 0.5 μm. The Ti–6Al–4V workpieces were washed gently in deionized water after laser treatment prior to conducting the electrochemical tests. The electrolytic solution used in the electrochemical tests is made if 0.05 M H_2SO_4 + 0.05 M NaCl. The cell used was composed of three electrodes. The Ti–6Al–4V workpiece was used as working electrode, a platinum wire was used as counter electrode, and a Ag/AgCl electrode was used as reference. The electrochemical experiments were performed using a EG&G PAR model 273A potentiostat–galvanostat controlled by a computer through the M352 corrosion software. EDS and SEM were carried out for

elemental study and morphology of the surfaces after the electrochemical oxidation. Before the SEM study, the sample surface was coated with gold to improve conductivity.

3. Results and discussion

3.1. *Results from potentiodynamic scans*

Table 1 shows the elemental composition of the Ti–6Al–4V alloy and Figure 1 shows the potentiodynamic scans of the untreated Ti–6Al–4V and laser treated alloy. The behaviour is typical of a noble alloy, where passivation occurs immediately after oxidation. Electrochemical parameters shown in Table 2 reveal that the corrosion potential of the laser treated alloy was 0.085 V as compared to −0.323 V for the untreated specimen. Hence, laser surface melting resulted in an anodic shift of the corrosion potential by 410 mV. The corrosion current density for the laser treated specimen as shown in Table 2 has a value of 0.168 μA cm^{-2} whereas the untreated corrosion current density exhibited a value of 0.371 μA cm^{-2}. The corrosion rate of the laser surface melted specimen was 5.74 μm y^{-1} compared to 12.7 μm y^{-1} for the untreated Ti–6Al–4V specimen. Hence, electrochemical corrosion parameters show an improvement in corrosion resistance by approximately a factor of two. However, analysis of the full potentiodynamic scans reveals a real time corrosion resistance
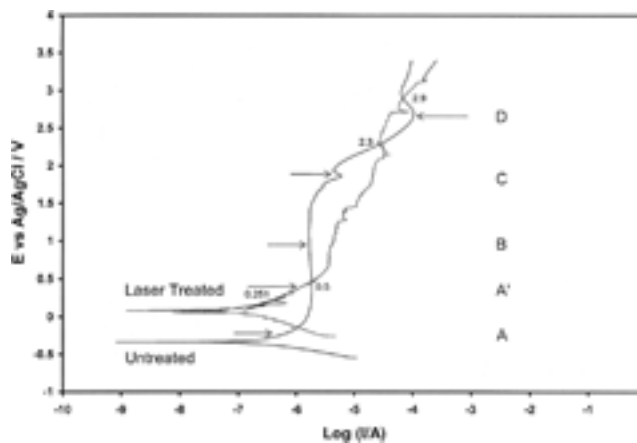

Fig. 1. Potentiodynamic scans of the untreated and laser treated Ti–6Al–4V alloy. Scan rate 0.166 mV s^{-1} in 0.05 M H_2SO_4 + 0.05 M NaCl. Arrows correspond to regions A, A′, B, C and D, respectively. The cross line correspond to 0.251 V. Two scans intersect at 0.5, 2.3 and 2.9 V, respectively.

Table 1. Elemental composition of Ti–6Al–4V alloy

Element	Ti	Al	V	Cu	Cr	Fe	O
Composition/wt %	Bal.	6	4	0.03	0.01	0.32	0.2

Table 2. Electrochemical corrosion parameters

Ti–6A1–4V	E_{corr} /mV	I_{corr} /μA cm^{-2}	Corrosion rate /μm y^{-1}
Untreated	−0.323	0.371	12.7
Laser treated	0.085	0.168	5.74

behaviour as compared to the theoretically extracted corrosion parameters in the Tafel region.

Figure 1 shows oscillation in the potentiodynamic scans of the laser treated specimen. Transient currents are very apparent around the corrosion potential. These oscillations are very frequent up to 0.5 V, after which the curve becomes less noisy. Repetitive transients show that the surface film is not stable and is subject to fast repetitive pitting and refilming. Moreover, this is indicative that the laser treatment does not yield a very homogenous surface. Although it improved the corrosion rate and corrosion potential, it caused severe film breaks even at open circuit potential. The untreated Ti–6Al–4V exhibited a passive region with a constant passive current of 1 μA, which was not observed for the laser treated specimen.

The laser treated specimen exhibited a continuously increasing current with current density values lower than the untreated specimen at very small overpotentials. Moreover, the laser treated specimen showed an abrupt upward change in slope at 251 mV (indicated by a cross line at 0.251 V in Figure 1). This is indicative that the laser surface tends to passivate at lower voltages as compared to the untreated sample. However, the passive area does not correspond to a constant current as in the case of the untreated sample, but may be described as semipassive as it showed a continuous increase in current. Rapid passivation upon oxidation is a quality required by the implants industry, since rapid metal passivation results in less ions released *in vitro* and hence less toxicity [19, 20]. At potentials higher than 0.5 V, which correspond to the intersection of the two potentiodynamic scans in Figure 1, the current densities of the laser treated samples were significantly higher than the untreated one up to 2.3 V, where the untreated specimen suddenly showed severe breakdown and refilming at 2.7 V. Above 2.9 V the laser specimen current densities again became higher again indicating greater susceptibility to corrosion.

3.2. *Results from ICP*

Electrolysis of the untreated and LSM specimen were carried out at the potentials corresponding to the arrows in Figure 1, regions A to D. Potentials A and A′ of the active region of the laser treated and treated were selected for electrolysis. Region B was selected to correspond to the region of relative passivity. Region C corresponds to the early stages of the breakdown of the passive film formed on the untreated sample. Region D is selected to determine the effect of polarization high potentials. The selected potentials for electrolysis are shown in Table 3.

Table 3. Selected potentials for electrolysis (V vs Ag/AgCl)

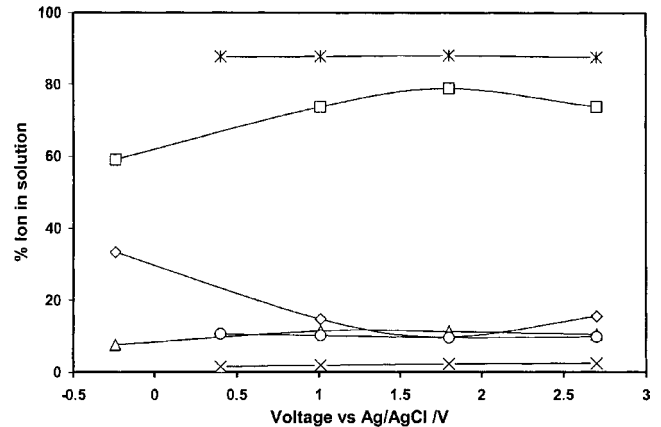|				
Untreated	−0.24 (A)	1.01 (B)	1.8 (C)	2.7 (D)
Laser treated	0.4 (A′)	1.01 (B)	1.8 (C)	2.7 (D)

Fig. 2. Plot of percentage Ti, Al, V of the untreated and laser treated specimen from ICP after electrolysis for 30 min at selected potentials. Untreated: (◇) Ti, (□) Al, (△) V; treated: (×) Ti, (∗) Al, (○) V.
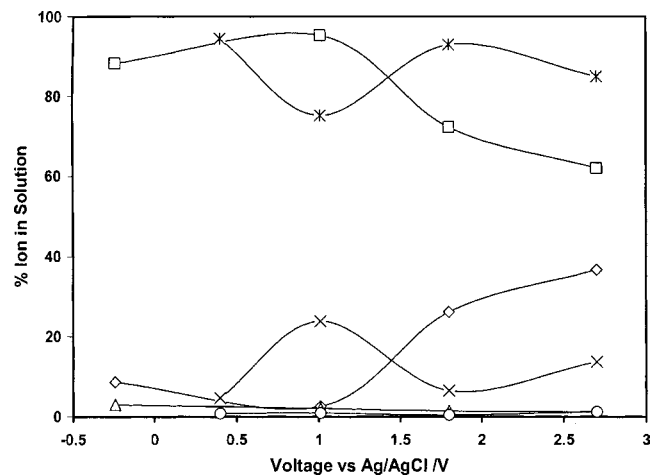

Fig. 3. Plot of percentage Ti, Al, V of the untreated and laser treated specimen from ICP after electrolysis at selected potentials for 2 h. Untreated: (◇) Ti, (□) Al, (△) V; treated: (×) Ti, (∗) Al, (○) V.

Figure 2 shows the ICP results for solution metal composition after 30 min electrolysis. Figure 3 shows the ICP results for solution composition after 2 h electrolysis. After 30 min in region A and A′, the titanium in solution dropped from 33.3% for the untreated specimen to 1.52% for the LSM specimen. Aluminium selective leaching, in the same region, increased from 59.0% to 87.8% and vanadium changed from 7.6% to 10.6%. Generally, the vanadium in all regions of both samples during 30 min electrolysis remained near 10%. Its lowest value occurred in region A which is the region of active dissolution before the formation of the passive film. Once the region of passivity is reached (region B) the percentage of vanadium in solution became independent of the applied potential. In region B the titanium in solution dropped from 14.7% for the untreated specimen to 1.9% for the laser treated specimen. For all other potentials of the laser treated specimen the percentage of titanium in solution remained near 2%. In region B, aluminium increased from 73.7% to 87.8% and remains near 88%

for the laser treated sample in regions B to D. Examination of region C for the untreated specimen showed that aluminium is 78.8% compared to 73.8% for regions B and D. It is clear that region C from Figure 3 corresponds to a peak. This peak is in the vicinity of the literature value of aluminium oxidation and might be due to active dissolution of aluminium at 1.8 V.

In contrast, the potentiodynamic scan of the LSM specimen shows no peak in region C. Moreover, Figure 2 shows that aluminium composition in solution reached a constant maximum value around 88% at all selected potentials. Figure 2 shows also that the titanium in solution decreased with laser treatment, aluminium increased and the vanadium, generally, remained unaffected.

Further electrolysis for 2 h showed very interesting features. The vanadium solution composition was in the range 3.02%–0.5%, a significant change compared to the range 7.64%–11.47% after 30 min electrolysis. The decrease in vanadium is due to the increased dissolution of other metals as a function of time. Vanadium reached a minimum of 0.5% in region C of the laser treated specimen. The titanium solution composition for the untreated specimen electrolysed for 30 min dropped from 33% to 8.7% after 2 h of electrolysis in region A. This was accompanied by a sharp increase in aluminium composition from 59% to 88%. Moreover, electrolysis in the passive region (B) showed a decrease of titanium composition from 14.7% at 30 min to 2% after 2 h, accompanied by an increase in aluminium composition from 74% to 95%. Hence, prolonged electrolysis in the passive region led to a drastic increase in aluminium solution composition. Titanium solution composition after 2 h electrolysis dropped from 8.68% for the untreated specimen in region A to 4.7% of the LSM specimen in region A′. Thus, laser treatment decreased the percentage of titanium leached in the active region during 2 h electrolysis. Similar results were observed for vanadium, where the corresponding concentrations dropped from 3.02% for the untreated specimen to 0.855% for the LSM specimen. Hence, if a Ti–6Al–4V is subjected to a small overpotential *in vivo* under similar solution conditions, it is expected that aluminium would leach the most in the surrounding tissues. Laser treatment would lower the solution composition of titanium at small overpotentials (region A′). Values at region D represent leaching under drastic corrosion potentials at 2.7 V, where it is noted from Figure 3 that vanadium composition remained constant at about 1.25% compared to titanium and aluminium.

3.3. Characterization of laser surface melting zone

Figure 4 shows the typical energy dispersive spectrum of the laser treated and electrochemically oxidized workpiece in solution. The first peak in the EDS spectrum corresponds to gold coating of the surface. Tables 4 and 5 show the EDS results of the untreated and laser
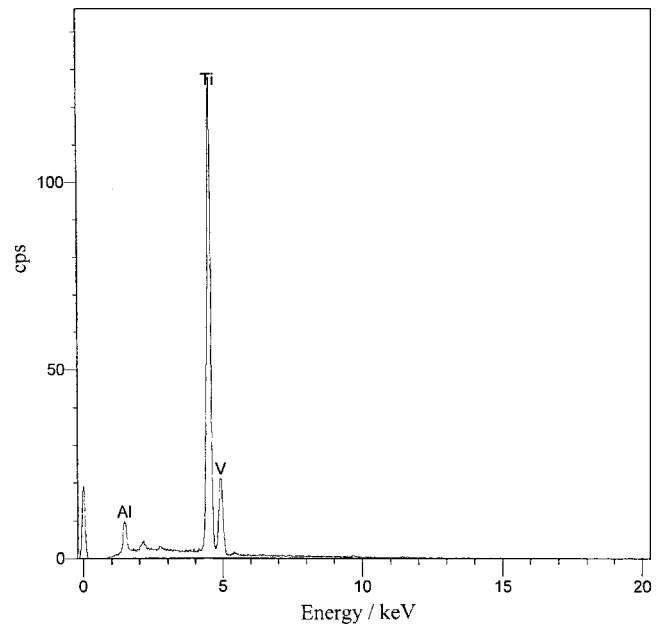

Fig. 4. Typical energy dispersive spectrum of the laser treated and electrochemically polarized Ti–6Al–4V alloy in solution.

Table 4. ESD after 30 min of electrolysis at selected potentials A/A′ to D

	Ti /%	Al /%	V /%
Untreated	Bal.	4.8	3.7
	Bal.	4.3	3.3
	Bal.	4.3	4.5
	Bal.	4.1	3.3
Laser treated	Bal.	3.8	4.8
	Bal.	3.2	4.3
	Bal.	3.4	4.5
	Bal.	3.1	4.1

Table 5. EDS after 2 h of electrolysis at selected potentials A/A′ to D

EDS	Ti /%	Al /%	V /%
Untreated	Bal.	0.3	3.7
	Bal.	0.4	3.7
	Bal.	0.4	3.7
	Bal.	0.4	3.8
Laser treated	Bal.	0.21	4.5
	Bal.	0.24	4.6
	Bal.	0.22	4.6
	Bal.	0.18	4.5

treated specimen after electrochemical oxidation in regions A–D (Figure 1) for different durations. It was observed that the degradation of aluminium at the surface after 2 h of electrochemical oxidation was evident in the laser treated specimen. During the first 30 min of oxidation the aluminium composition changed only slightly within 1%. The vanadium percentage also remained within 1% with some enrichment of titanium. The temperature attained during laser melting is extremely high. Attainment of such high temperatures
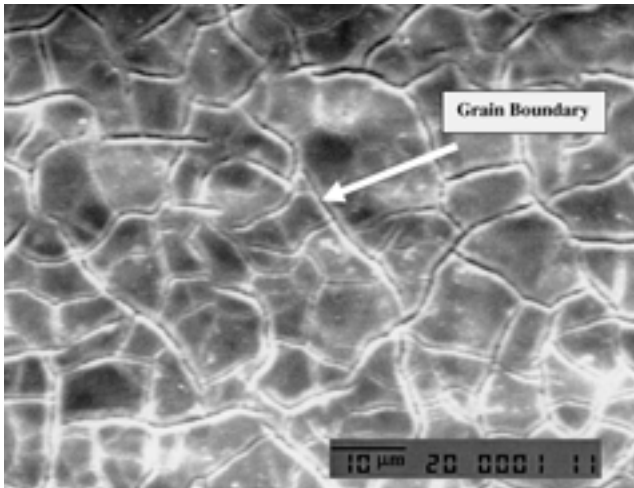
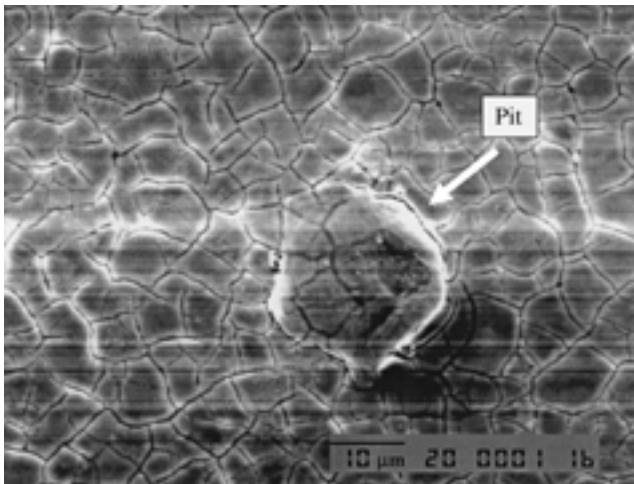Fig. 5. SEM micrograph of the Ti–6Al–4V surface showing grains boundaries and no pitting.

Fig. 6. SEM micrograph of the laser treated surface after 30 min of electrochemical polarization at 2.7 V showing pit initiation.
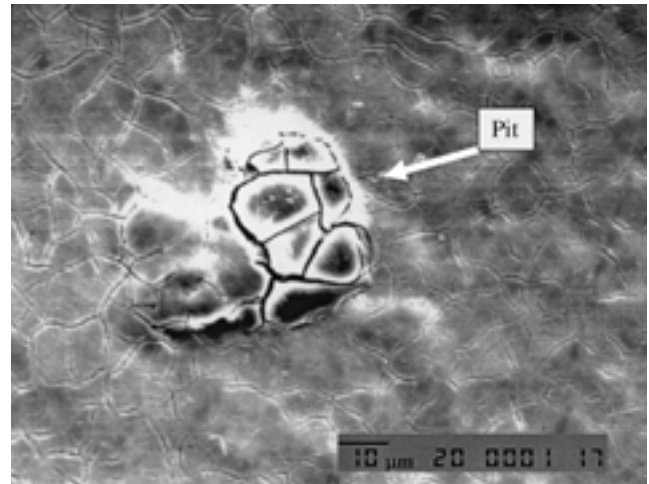

Fig. 7. SEM micrograph of the laser treated surface after 120 min of electrochemical polarization at 2.7 V showing pit site formation.

in the pit site does not occur; in which case, the existence of corrosion product in the pit site is not observed.

4. Conclusion

The combined analysis of electrochemical, ICP, SEM and EDS leads to the following conclusions:
 (i) Laser treatment leads to a decrease in the corrosion rate of Ti–6Al–4V but yields an unstable current indicating continuous dissolution and passivation.
 (ii) Aluminium was found to leach out selectively in solution at all selected potentials. A maximum of 94% was reached after 2 h in the passive region at 1.01 V.
(iii) Titanium in the passive region B, was found to leach out with a percentage of 23.8% for the laser treated specimen compared to 2.64% for the untreated one after 2 h of electrolysis.
(iv) The higher percentage of aluminium in solution correlates with the degradation of aluminium near the surface of the substrate material as observed from EDS results. This is particularly true for the laser treated surfaces after 2 h of electrolysis.
 (v) Local pitting with shallow depth and irregular shape occurred.

Acknowledgement

coupled with very high cooling rates usually results in metastable microstructures. LSM usually leads to the resolidification of the melted zone in epitaxial form which manifests in an unstable current profile [21]. Moreover, during the laser treatment process aluminium in the surface region melts and evaporates earlier, which in turn, results in aluminium to concentrate locally in the surface vicinity of the substrate material and depletion from the surface in agreement with early work [22]. SEM examination of the alloy surface after controlled potential electrolysis was carried out for each potential region.

Figure 5 shows a sample SEM of the untreated Ti–6Al–4V surface. The grain boundaries are evident in the Figure. Figures 6 and 7 show sample SEM micrographs of laser treated surface after 30 min and 2 h of electrochemical polarization at 2.7 V. Some small local pitting is evident as marked on Figures 6 and 7, for the laser treated sample. The pits generally appear to be irregular in shape and shallow. Consequently, secondary pitting

References

1. K.G. Budinski, *Wear* **151** (1991) 203.
2. I.J. Polmear, 'Light alloys, metallurgy of light metals' (Edward Arnold, London, 2nd edn, 1989).
3. T. Shibata and Y-C. Zhu, *Corros. Sci.* **37**(2) (1995) 253.
4. J. Lausmaa, *J. Electron Spectrosc. Relat. Phenom.* **81**(3) (1996) 343.

5. M.G.S. Ferreira, R. Li and R. Vilar, *Corros. Sci.* **38** (1996) 2091.
6. S. Yerramareddy and S. Bahadur, *Wear of Mater*. **8**(1) (1991) 531.
7. O.V. Akgun and O.T. Inal, *J. Mater. Sci.* **29** (1994) 1159.
8. K-H. Zum Gahr and J. Schneider, *Ceramics International* **26** (2000) 363.
9. W.M. Steen, *in* Proceedings of the second European conference on 'Laser Treatment of Materials', Bad Nauheim, FRG (1988), p. 60.
10. D.S.Ghanamothu, *in* E.A. Metzbower (Ed.), 'Applications of Lasers in Materials Processing', (ASM, Cleveland, OH, 1979), p. 177.
11. S. Kumar and M.K. Banerjee, *Surf. Eng.* **17** (2001) 483.
12. G. Peto, A. Karacs, Z. Paszti, L. Guczi, T. Divinyi and A. Joob, *Appl. Surf. Sci.* **186** (2002) 7.
13. Y. Nakashima, D.H. Sun, L.E. Chun, M. Trindade, Y. Song, W.J. Maloney, S.B. Goodman, D.J. Schurman and R.L. Smith, *J Bone Joint Surg*. **81B** (1999) 155.
14. D.W. Howie, S.D. Rogers, M.A. McGee and D.R. Haynes, *Clin. Orthop.* **329** (1996) S217.
15. C.N. Martyn, C. Osmond, J.A. Edwardson, D.J.P. Marker, E.C. Harris and R.F. Lacey, *Lancet* **1** (1989) 59.
16. H. Meiri, E. Banin, M. Roll and A. Rousseau, *Neurobiol.* **40** (1993) 89.
17. R.G. Miller, F.C. Kopfler, K.C. Kelty and J.A. Stober, N.S. Ulmer, *J. Am. Water Works Assoc.* **76** (1984) 84.
18. M. Khaled, B.S. Yilbas and J. Shirokoff, *Surf. Coat. Technol.* **148** (2001) 46.
19. H.F. Hildebrand and J.C. Hornez, *in* J.A. Helson and H.J. Breme (Eds), 'Metals as Biomaterials' (J. Wiley & Sons, Chichester, UK, 1998), p. 265.
20. H. Zitter and H. Plenk, *J. Biomed. Mat. Res.* **21** (1987) 881.
21. P.G. Moore, *in* E. McCafferty, C.E. Clayton and J. Oudar (Eds) Proceedings of the international symposium on 'Fundamental Aspects of Corrosion Protection by Surface Modification', (The Electrochemical Society, 1984), p. 102.
22. B.S. Yilbas, J. Nickel, A. Coban, M. Sami, S. Shuja and A. Aleem, *Wear* **212** (1997) 140.